J Solid State Electrochem (2010) 14:231–240
DOI 10.1007/s10008-009-0812-7

ORIGINAL PAPER

Ru oxide/carbon fabric composites for supercapacitors

Xiaorong Liu · Peter G. Pickup

Received: 18 November 2008 / Revised: 9 February 2009 / Accepted: 20 February 2009 / Published online: 11 March 2009

Abstract Ru oxide/carbon fabric composites (Ru oxide/CF) were prepared by impregnating carbon fabric (CF) with a hydrous RuO_2 suspension. Their properties were characterized by scanning electron microscopy, impedance spectroscopy, cyclic voltammetry, and constant current discharging. Specific capacitance increased with increasing loading of Ru oxide. The apparent average specific capacitance of the Ru oxide component reached 1,085 F g^{-1} for a 9.15% loading, with a peak of 1,984 F g^{-1} at approximately 0.3 V vs Ag/AgCl. The presence of Ru oxide decreases the ionic resistance of the CF and appears to increase its specific capacitance by generating additional electroactive surface functionality.

Keywords Supercapacitor · Carbon fabric · Ru oxide · Impedance · Specific capacitance

Introduction

In recent years, supercapacitors have become an increasingly active research subject due to their applications in hybrid vehicles, backup power sources, portable electronic devices, digital communication, and microelectronic devices [1–4]. Carbon-based materials, such as activated carbon, carbon nanotubes, carbon blacks, carbon aerogels, and carbon fibers, are favorite materials for supercapacitors because of their high surface areas, good conductivity, low price, and high stability [1, 5]. However, these kinds of supercapacitors provide low volumetric energy and power density, and this limits their applications in fields that require high volumetric capacitance, such as microrobots, implantable medical devices, and portable electronic devices.

Metal oxides, such as Ru oxide, Ir oxide, and Mn oxide, have been attracting great interest due to their high gravimetric and volumetric capacitances. Among these metal oxides, hydrous Ru oxide currently provides the best performance [6–8]. Zheng and Jow's [9] 1995 report that the specific capacitance of Ru oxide could be increased to 720 F g^{-1} by use of a sol-gel synthesis method renewed interest in the use of Ru oxide in supercapacitors [10–17] and has led to the development of many composite materials aimed at maximizing the utilization of the expensive Ru component [18–38]. Hu and Chen have reported a specific capacitance of 1,580 F g^{-1} for the Ru oxide component of a composite with activated carbon [39] and suggest that a specific capacitance of 2,000 F g^{-1} or more is theoretically possible [24, 39].

Here, we report on novel Ru oxide composites with high surface area carbon fabric (CF; Spectracarb 2225). CF is an attractive electrode material for supercapacitors because of its high specific capacitance and the fact that it is fabricated into a self-supporting and highly porous form with good electronic conductivity [40–45]. Its modification with pseudocapacitive materials can provide higher specific capacitances and can increased energy and power densities [46, 47]. Ru oxide is a particularly attractive modifier because of its very high specific capacitance and rapid charge/discharge characteristics [8]. The purpose of this work was to develop a suitable method for preparing composites of Ru oxide with carbon fabric and to characterize the specific capacitances of these materials and their performance characteristics in supercapacitors. The question of whether dispersion of ruthenium oxide on a carbon fabric support can increase its specific capacitance has also been addressed.

X. Liu · P. G. Pickup (✉)
Department of Chemistry, Memorial University of Newfoundland, St. John's, Newfoundland A1B 3X7, Canada
e-mail: ppickup@mun.ca

Experimental

Preparation of Ru oxide/CF composites Hydrous ruthenium oxide power (0.01–0.5 g), prepared by a sol-gel method as described previously [7] and annealed for 3 h at 150 °C in air, was dispersed in water (10–100 mL) by sonication for approximately 30 min. For low loadings of Ru oxide (< 30%), Spectracarb 2225 carbon fabric (Engineered Fibers Technology; typical size 4×4 cm) that had been dried for 24 h at 150 °C was immersed in this suspension for approximately 30 min, then dried for approximately 10 min at 150 °C. This immersion/drying procedure was repeated until the targeted mass loading of Ru oxide was reached. Finally, the composite was dried for 1–2 h at 150 °C to obtain a stable mass. The increase in mass relative to the original mass of the CF was used to estimate the Ru oxide loading and for calculation of specific capacitances due to the Ru oxide. For high loadings of Ru oxide (>30%), the Ru oxide suspension was added dropwise to a 2×4-cm piece of CF on a hot plate at approximately 50 °C.

Thermogravimetric analysis (TGA) of a sample with a 19.7% mass increase gave an average (seven measurements) residual RuO_2 mass of 17.6%, indicating that good control of the Ru oxide loading was achieved. A 9.1% mass sample gave a residual RuO_2 mass of 7.5% (average of five measurements). TGA could not be used to determine the hydration number of the Ru oxide in the composite because the mass loss due to dehydration overlapped with loss of carbon due to oxidation by the Ru oxide. However, TGA of the Ru oxide alone annealed at 150 °C indicated a degree of hydration of $RuO_2{\cdot}0.5H_2O$ that is consistent with the literature value [6]. X-ray diffraction showed the oxide to be amorphous; however, annealing at 250 °C produced the characteristic pattern for RuO_2, as previously reported [9].

Physical characterization Scanning electron microscopy (SEM) was performed with an FEI Quanta 400 environmental SEM.

Supercapacitors Supercapacitors were constructed by sandwiching a Nafion® film (NRE211, DuPont) between two equivalent 1-cm^2 Ru oxide/CF electrodes. Two titanium plates built into polycarbonate blocks were used as current collectors. A piece of carbon fiber paper (Toray™ Carbon Paper, TGP-H-090) was placed between each titanium plate and electrode to minimize the contact resistance. The assembly was immersed in a 1-M H_2SO_4 electrolyte in air.

Electrochemical characterization Three-electrode and two-electrode configurations were used for characterizing the properties of electrodes. For the three-electrode configuration, two identical Ru oxide/CF composite electrodes were used as the working electrode and counter electrode, respectively, with an Ag/AgCl reference electrode immersed in the external 1-M H_2SO_4 electrolyte. In contrast, the reference electrode lead of the potentiostat was connected to the counter electrode in the two-electrode (supercapacitor) configuration.

Cyclic voltammetry and constant current discharging experiments were conducted by using an EG&G 273A potentiostat. For constant current discharging, the supercapacitors were charged at 1 V for a period of 5 min, then discharged to 0 V. Specific capacitances from both types of experiment are reported as the average over the full potential ranges employed. For cyclic voltammetry, averages from the anodic and cathodic scans are reported.

Impedance spectroscopy measurements were performed with a Solartron 1286 Potentiostat and 1250 Frequency Response Analyzer. The frequency range was from 10 kHz to 10 or 5 mHz, with an amplitude of 10 mV and 0.5 Vdirect current bias potential.

Results

Scanning electron microscopy

Ru oxide and Ru oxide/CF composites were characterized using SEM. Figure 1a shows an SEM image of a sample of pure hydrous Ru oxide, which was annealed at 110 °C and had a specific capacitance of 678±69 F g^{-1}. It had a porous structure with visible grain and pore sizes ranging from below 0.1 μm to approximately 1 μm. Figure 1b shows an image of a 9.09% Ru oxide/CF composite. The carbon cloth consists of approximately 10-μm-diameter porous cylindrical fibers. Its surface is rough, providing anchor sites for the Ru oxide particles. The Ru oxide phase evenly distributes at the surface, and its particle sizes range from tens to hundreds of nanometer. Figure 1c, d shows increasing loadings of Ru oxide on CF. As the loading was increased, increasingly large clumps of Ru oxide were observed.

Although Ru partially covered the surface of the CF, the fraction of surface covered by Ru oxide is insignificant compared to the approximately 2,500 m^2 g^{-1} surface area of the CF. This aids in calculating the specific capacitance of the Ru oxide component in that it should be acceptable to neglect any change in the specific capacitance of the CF due to blocking of the surface by Ru oxide.

Electrochemistry of the electrodes (three-electrode mode)

The electrochemistry of the CF and Ru oxide composite electrodes was characterized by cyclic voltammetry and impedance spectroscopy using a three-electrode configuration

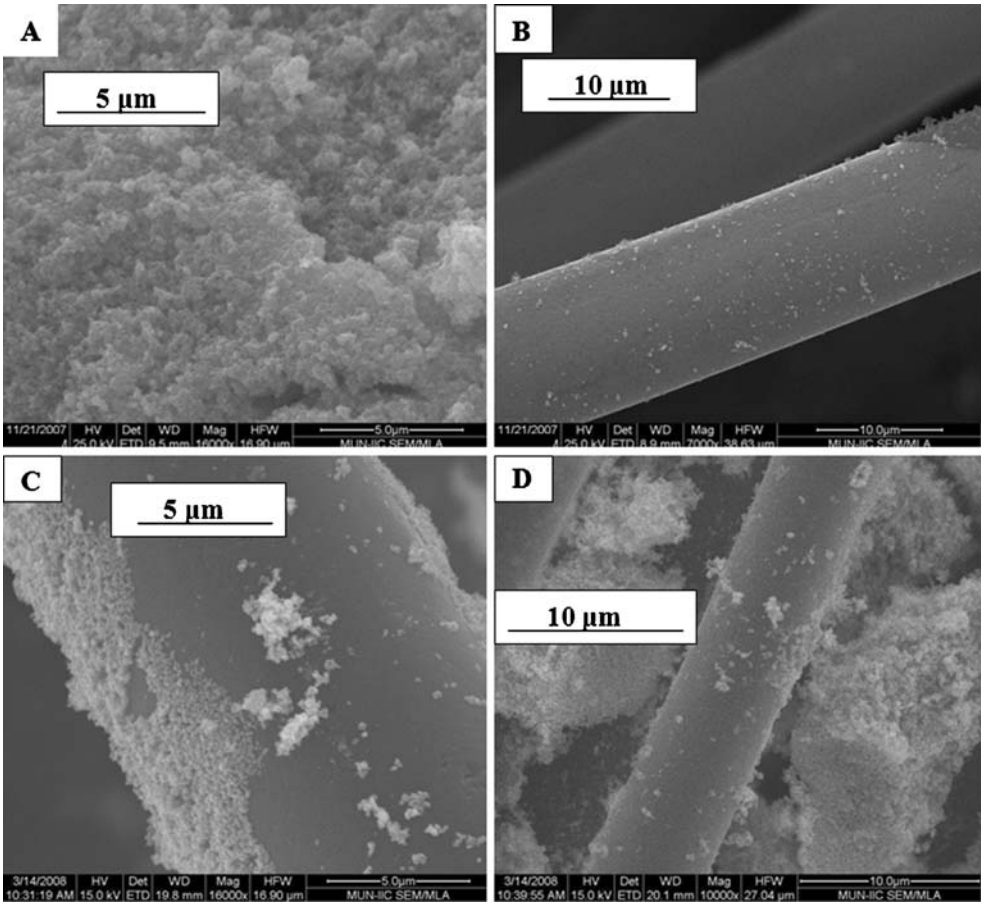

Fig. 1 SEM images of Ru oxide (**a**) and Ru oxide/CF composites with Ru oxide loadings of 9.09% (**b**), 19.7% (**c**), and 59.2% (**d**)

in which the potential of one of the electrodes (the working electrode) was controlled relative to an Ag/AgCl reference electrode. Figure 2 shows cyclic voltammograms of an unmodified CF electrode and a Ru oxide/CF composite electrode with a 9.15% mass loading of Ru oxide. The current axis of the voltammograms has been converted to a specific capacitance axis by dividing by the scan rate and the mass of the electrode. Also shown in Fig. 2 is a specific capacitance vs potential plot for the Ru oxide component of the electrode, calculated from the other two curves by subtracting the CF capacitance from the capacitance of the composite at each potential. It should be noted that the capacitances measured here include both double-layer capacitances due to the carbon and possibly Ru oxide surfaces, as well as Faradiac pseudocapacitances due to the Ru oxide and functional groups on the carbon.

It is clear from Fig. 2 that the Ru oxide increases the specific capacitance of the CF at all potentials, with the largest increase seen as a broad peak centered at approximately +0.34 V. The average specific capacitance of the CF over the −0.2 to 0.8 V potential range was 195 F g^{-1}, while the Ru oxide/CF composite exhibited an average value of 277 F g^{-1} over the same range. The calculated average specific capacitance of the Ru oxide component was 1,085 F g^{-1}, with peak capacitances of 1,980 and

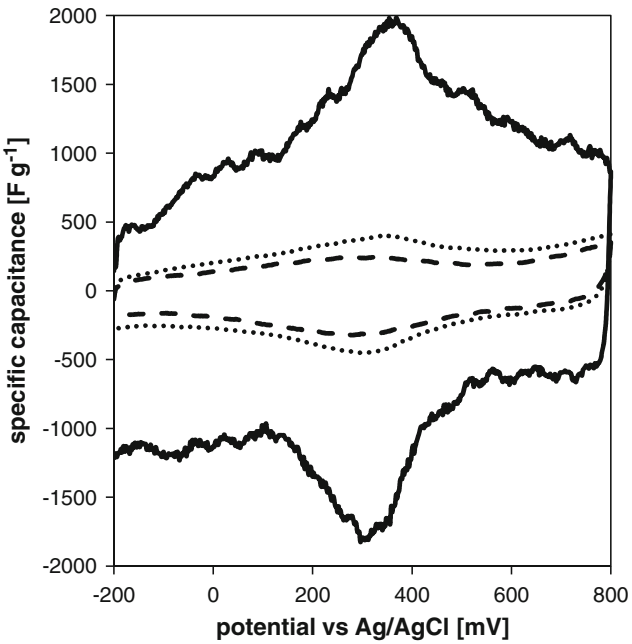

Fig. 2 Cyclic voltammograms (5 mV s^{-1}) of CF (*dashed*) and a 9.15% Ru oxide/CF composite (*dotted*). The *solid line* is the calculated specific capacitance of the Ru oxide component of the composite electrode

1,820 F g^{-1} seen at 0.368 and 0.296 V, respectively, on the forward and backward scans. An average specific capacitance of 1,084 F g^{-1} based on Ru oxide was obtained by discharging the electrode from +1 to 0 V at 10 mA.

The potential dependence of the specific capacitance of the CF and 9.15% Ru oxide/CF composite was also investigated by impedance spectroscopy using the three-electrode configuration. Results, including the calculated specific capacitance of the Ru oxide component at each potential, are shown in Fig. 3. There is a clear peak due to the Ru oxide at 0.3 V. The maximum specific capacitance for the Ru oxide component reached 1,480 F g^{-1}.

CF supercapacitors

The performances of CF supercapacitors were measured by cyclic voltammetry and impedance spectroscopy. The specific capacitance of CF was found to increase with time in 1-M H_2SO_4 electrolyte, as shown by the voltammograms in Fig. 4 and plotted in Fig. 5. The specific capacitance increased from 158 to 237 F g^{-1} during the first 96 h but then remained constant. Furthermore, Fig. 3 shows a pair of redox peaks due to functional groups on the carbon cloth, which increase with soaking time.

Slow wetting of the carbon fibers was considered as a possible explanation for the increase in capacitance. CF has a very narrow pore-size distribution and its porosity (mainly <2 nm) is mainly located on the surface, providing good accessibility for electrolyte [5]. However, air could be trapped in pores when the electrodes are immersed in the electrolyte solution. In order to prevent this, electrolyte was impregnated into the electrodes in an evacuated flask before assembly in the cell. As shown in Fig. 5, this did not improve the initial capacitance nor significantly influenced the growth in capacitance with time. It was also found that the capacitance did not change with time in LiOH(aq) (Fig. 5), further indicating that trapped air was not an issue.

The change in the shape of the voltammogram with time (Fig. 4) suggests that the increase in capacitance is related to changes in the surface functionality of the CF. The initial

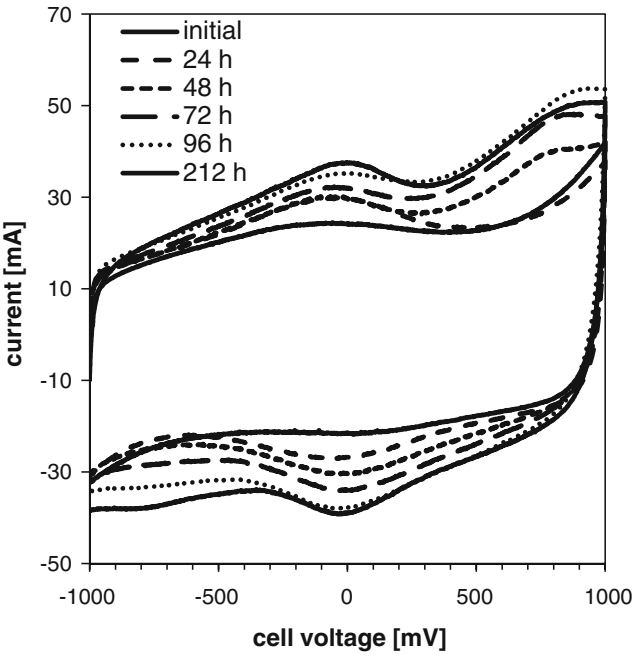

Fig. 4 Cycle voltammograms (20 mV s^{-1}) of a CF supercapacitor with 13.4- and 13.7-mg electrodes

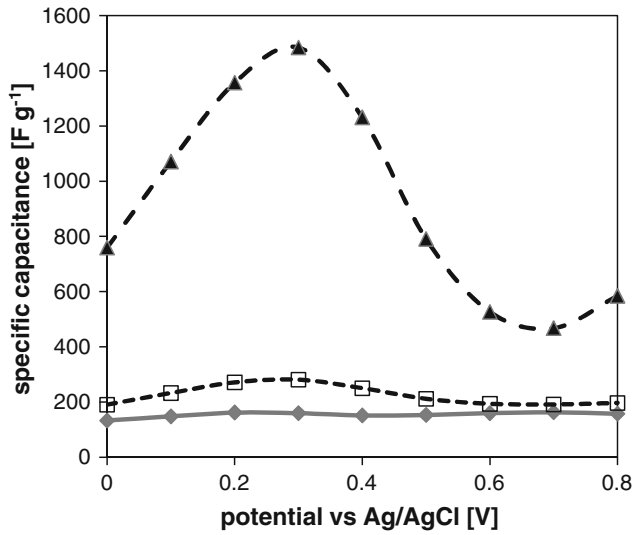

Fig. 3 Potential dependences of the specific capacitances from impedance measurements for CF (*diamonds*), a 9.15% Ru oxide/CF composite (squares), and the Ru oxide component of the composite (triangles)

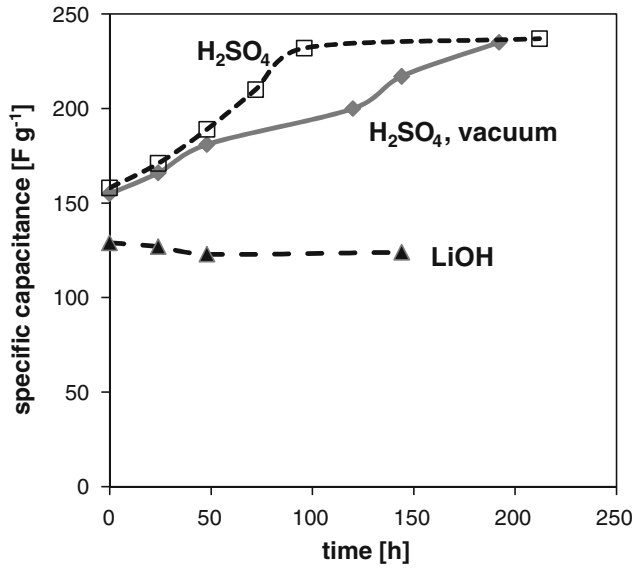

Fig. 5 Specific capacitance *vs.* soaking time for CF supercapacitors in 1 M H_2SO_4, with (*diamonds*) and without (*squares*) application of a vacuum during impregnation of the electrodes with electrolyte, and in 2 M LiOH (*triangles*) without vacuum impregnation

voltammogram is quite featureless with only very small peaks at approximately 0 V due to the electrochemistry of surface redox groups. However, these peaks grew significantly with time, providing a large contribution to the increase in capacitance. Additional irreversible waves also developed at approximately +0.9 and −0.9 V (these are both due to the same process since this was a symmetric device).

CF has various surface functional groups, such as phenolic, hydroxyl, carboxyl, carbonyl, and quinone groups [5]. Various surface redox processes have been proposed to explain the peaks (generally at approximately 0.3 V vs saturated calomel electrode (SCE) in aqueous acid) seen in voltammograms of carbon in aqueous solutions and the increases in capacitance observed following oxidation of carbon samples [41, 48–50]. The broadness of the peaks indicates the existence of a number of different processes. A series a quinone–hydroquinone-type couples based on structures similar to that shown in Scheme 1 appear to be the most reasonable candidates. These would explain the peaks seen at a cell voltage of approximately 0 V (both electrodes at approximately 0.3 V vs SCE) in Fig. 4. The growth of these peaks with time is likely due to oxidation of the carbon surface by oxygen since air was not excluded from the cell. The irreversible peaks that appear at approximately ±0.9 V may be due to oxidation of isolated >CH–OH groups.

Since the changes in capacitance shown in Figs. 4 and 5 could cause errors when comparing the capacitances of unmodified carbon fabric with the capacitances of Ru oxide/CF composites, it is important to make comparisons following similar soaking times. Testing of five unmodified CF cells by cyclic voltammetry after 17 h of soaking time gave an average specific capacitance of 175±6 F g^{-1}, indicating that excellent reproducibility could be obtained.

Ru oxide/CF composite supercapacitors

Figure 6 shows voltammograms of symmetric supercapacitors with various loadings of Ru oxide on the CF electrodes. The Ru oxide/CF composites show good capacitive behavior over the −1 to 1 V potential range, with specific capacitances (C_S) increasing with Ru oxide loading, as documented in Table 1. Specific capacitances obtained from these voltammograms showed good reproducibility. For example, an average specific capacitance of 237±5 F g^{-1} (relative standard deviation=2.2%) was obtained for six cells containing a 10.0% Ru oxide/CF composite.

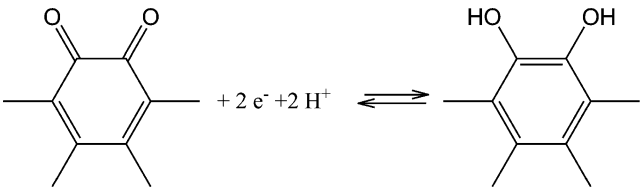

Scheme 1 Proposed process occurring at ~0.3 V on carbon

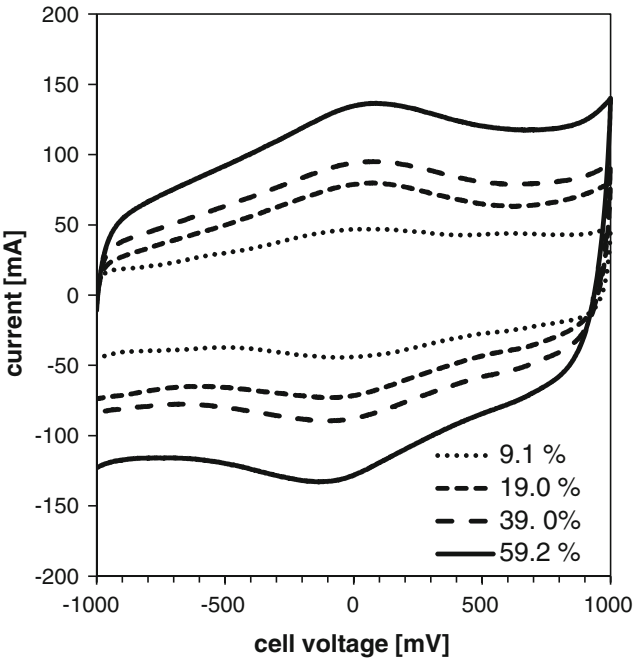

Fig. 6 Cyclic voltammograms (20 mV s^{-1}) for Ru oxide/CF supercapacitors with the specified Ru oxide loadings

Also shown in Table 1 are apparent specific capacitances for the Ru oxide component of each composite, calculated by subtracting the contribution to the total capacitance from the CF support. Compared to pure Ru oxide tested under similar conditions, the specific capacitance based on Ru oxide was increased from 678±69 F g^{-1} [7] to 978±60 F g^{-1} for the composite with a 9.09% loading. This represents an apparent 44% increase in electrochemical utilization of the Ru oxide. However, the specific capacitance based on Ru oxide, and hence the apparent Ru oxide utilization, was found to decrease with increasing Ru oxide loading. Possible reasons for this effect are explored in the "Discussion."

The Ru oxide/CF composite supercapacitors showed excellent long-term stability. A device with the 10.0% Ru oxide/CF composite exhibited no loss of capacitance over 10,000 continuous charge–discharge cycles between 0 and 1 V at 0.1 A.

As illustrated in Fig. 7, Nyquist plots of both the CF and Ru oxide/CF supercapacitors showed high-quality porous electrode behavior, with approximately 45° linear regions at high frequency and almost vertical regions at low frequency. Equivalent series resistances (*ESR*) of the supercapacitors, measured at 10 kHz, are listed in Table 2. All cells had *ESR* values close to 100 mΩ with the composites showing slightly lower resistances than the unmodified CF. Table 2 also lists ionic resistances (R_{ion}) for the electrodes, calculated from [7]:

$$R_{ion} = 3[Z'(f) - ESR] \quad (1)$$

Table 1 Specific capacitances (C_S) of Ru oxide/CF composites after 17 h in 1 M H_2SO_4

Ru oxide loading [%]	Electrode mass [mg]	C_S [F g^{-1}] at 10mA discharge	C_S [F g^{-1}] by CV at 20mV s^{-1}	C_S [F g^{-1}] of the Ru oxide[a]
9.09	14.4+14.5	280	248	978±60
19.7	19.9+19.9	264	294	779±24
39.0	21.0+21.5	383	340	599±9
59.2	26+26.5	427	402	559±4

[a] Based on C_S=175±6 F g^{-1} for the CF and C_S values from CV

where *Z′(f)* is the real part of the impedance at the characteristic frequency (*f*), defined by Miller [51] (see below).

R_{ion} values were lower for the composites than for CF alone and increased with increasing Ru oxide loading. The most likely explanation for this is that the presence of Ru oxide increases the hydrophilicity of the carbon and promotes wetting, while also physically blocking (or restricting) access of electrolyte to parts of the carbon surface.

Table 2 also lists specific capacitances determined from the limiting low-frequency capacitances obtained from impedance measurements. They parallel the voltammetric results shown in Table 1, although all values are lower. The difference can be ascribed to the potential range used in each type of experiment, −1 to 1 V for cyclic voltammetry and 0.5±0.014 V for impedance spectroscopy. It can be seen from the voltammograms in Fig. 6 that the capacitance passes through a minimum at cell voltages close to the average value of 0.5 V used the impedance measurement. It is also well known that the small amplitude excitation used in impedance spectroscopy yields significantly lower capacitances for electrochemical systems than the wide amplitude excitation in cyclic voltammetry, although the reason is not fully understood.

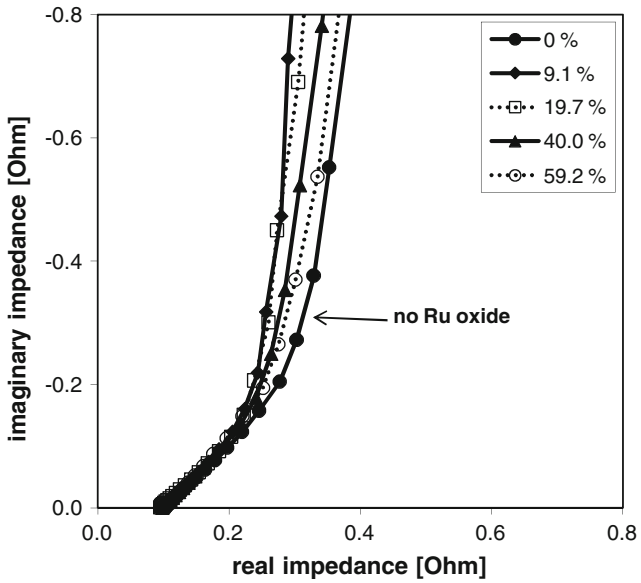

Fig. 7 Complex plane (Nyquist) plots for CF and Ru oxide/CF supercapacitors with Ru oxide loadings as indicated

Miller [51] defined a characteristic frequency (*f*) for a supercapacitor as the frequency when the phase angle of the impedance reaches 45°. The imaginary and real parts of the impedance have equal values at this frequency. The reciprocal of the characteristic frequency was termed the characteristic response time (τ), and this approximates the minimum charging–discharging time of the device for pulse operation. Energy (*E*) and power (*P*) densities estimated at the characteristic frequency by using the following equations provide a convenient way of making rapid comparisons between devices [51].

$$E = CV^2/2m \tag{2}$$

where *V* is the rated voltage of the capacitor; *m* is the device mass; $C=-1/(2\pi fZ'')$, and Z'' is the imaginary impedance at *f*.

$$P = E/\tau \tag{3}$$

Energy and power densities calculated with these equations are listed in Table 2. It can be seen that the presence of Ru oxide increases the energy density greatly, by more than 160%, but that use of loadings above 20% offers no further benefits. Power density was increased by approximately 10% for 9.09% Ru oxide, but higher loadings gave decreased power densities. The optimum Ru oxide loading is therefore between 10% and 20%.

In an attempt to further improve the performances of the supercapacitors, Nafion® was added to the electrodes. This has been found to significantly improve the performances of Ru oxide electrodes in supercapacitors [7], where it allows the establishment of proton conduction pathways, decreasing the electrode ionic resistance and increasing the utilization of the Ru oxide.

A Ru oxide/CF supercapacitor with 3.6% Nafion® added to both electrodes (by immersion in 1.5% Nafion solution for several minutes) was characterized by cyclic voltammetry, impedance spectroscopy, and constant current discharging. Figure 8 compares results with those from a similar supercapacitor with no Nafion added to the electrodes. The Nyquist plots (Fig. 8a) show that the addition of Nafion increases the resistance of the electrodes by a factor of

Table 2 Summary of impedance results for CF and Ru oxide/CF supercapacitors

Ru oxide loading	τ [s]	$Z'(f)$ [mΩ]	ESR [mΩ]	R_{ion} [mΩ]	C_S [F g^{-1}]	C_S of Ru oxide [F g^{-1}]	Energy density [W h kg^{-1}]	Power density [kW kg^{-1}]
0	1.18	313	108	615	144±8.7		3.1	9.4
9.09%	1.83	248	99	446	203	798±87	5.6	10.3
19.7%	3.08	249	97	456	249	678±35	8.1	9.5
39.0%	4.31	268	100	505	319	593±17	8.0	6.7
59.2%	6.72	278	99	537	392	564±7	8.1	4.3

approximately 4, while both impedance and voltammetry (Fig. 8b) show an increase in capacitance. The specific capacitance was increased by 31% (from 248 to 326 F g^{-1}) based on cyclic voltammetry. The increase in capacitance is likely due to better wetting of the carbon surface when it is coated with a thin Nafion layer, while the increase in resistance is probably due to the presence of Nafion in the ion conducting channels (pores) since Nafion has a lower ionic conductivity than 1 M H_2SO_4.

Constant current discharge experiments (Fig. 8c) and the derived Ragone plots (Fig. 8d) showed better performances for the device without Nafion in the electrodes, indicating that the effects of the increased resistance with Nafion outweighed the benefits of the increased capacitance. The best energy density was 8.1 W h kg^{-1} at 10 mA, while the best power density was 9.8 kW kg^{-1} at 1.0 A. These are similar to the energy and power densities estimated by impedance (Table 2), although a quantitative comparison is not possible since the values from the constant current experiments are for full discharge, while the values from impedance are supposed to be representative of pulse power performance [51]

Discussion

The results reported here for Ru oxide/CF composites parallel those reported for composites of Ru oxide with a wide variety of different carbons. A comparison of specific capacitances is presented in Table 3. The Ru oxide/CF composite with 9% Ru oxide has the best specific capacitances reported for such a low loading. This is due to the high specific capacitance of the CF since the specific capacitance of the Ru oxide component (978 F g^{-1}) was not as high as some literature values. Although obtaining maximum utilization of the expensive Ru component is

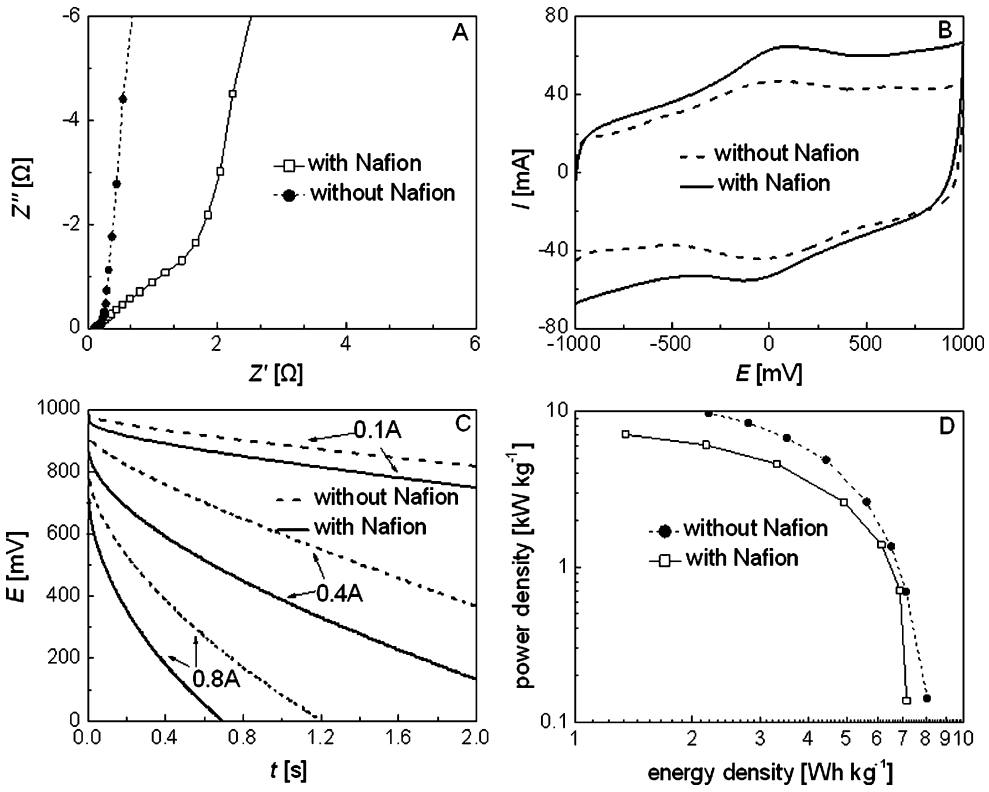

Fig. 8 Effect of Nafion® addition on the properties of a 9.09% Ru oxide/CF supercapacitor. **a** Nyquist plots; **b** cyclic voltammograms at 20 mV s^{-1}; **c** constant current discharge plots; **d** Ragone plots

Table 3 Comparison of specific capacitances with literature values

Type of carbon; area [m^2 g^{-1}]	Ru oxide loading	C_S of composite [F g^{-1}]	C_S of Ru oxide [F g^{-1}]	Reference
Fabric; 2,500	9%	280	978	This work
Fiber; 180	9%	~70	~500	[37]
Activated; 750	10%	147	1,200	[24]
Activated; 750	10%	250	1,580	[39]
Fiber; 13	33%	330	1,017	[34]
Mesoporous; 1,000	40%	633	742	[53]
Fabric; 2,500	40%	382	599	This work
Fiber; 180	40%	~190	440	[37]
Black; 248	50%	407	863	[22]
Fabric; 2,500	59%	427	559	This work
Activated; 750	60%	352	567	[24]
Black; 1,480	60%	647	988	[28]

important, it is more important from an application point of view to obtain the best performance on a Ru mass basis. The low-loading (9–20%) Ru oxide/CF composites are therefore particularly attractive. As shown in Table 2, outstanding performances can be obtained in supercapacitors with small amounts of Ru.

The specific capacitances of the Ru oxide component of the Ru oxide/CF composites decreased significantly with increasing loading (Table 1), as has commonly been reported for other Ru oxide/carbon composites (Table 3). From the micrographs in Fig. 1, it can be seen that use of higher loadings caused clumping of the Ru oxide and increases the average distance to a carbon fiber. It is therefore understandable that some of the Ru oxide becomes inactive due to poor electrical contact with the carbon fabric.

Some literature reports show that high Ru oxide specific capacitances can be maintained at high loadings (Table 3). Most notable is the 988 F g^{-1} reported in [28] for 60% Ru oxide on Ketjen Black (KB). This work employed KB that had been oxidized with nitric acid to increase its hydrophilicity, as well as fumed silica to form a network of nanopores when removed with NaOH. The resulting composite had a specific capacitance of 647 F g^{-1}.

Composites of Ru oxide with carbon are of significant fundamental interest as well as being potentially useful in supercapacitors. By dispersing Ru oxide on carbon, the fraction of Ru sites that are electrochemically active can be maximized, and it is possible to approach a measurement of its intrinsic specific capacitance. Theoretically, for $RuO_2 \cdot 0.5H_2O$ (molar mass=142 g mol^{-1}) and a potential window of approximately 1 V, the specific capacitance (C_S) per electron is approximately 680 F g^{-1}. Thus, if each Ru site can store two electrons in a transition from Ru(V) to Ru (III), for example, the theoretical specific capacitance is approximately 1,360 F g^{-1}, while a Ru(VI) to Ru(III) transition would provide approximately 2,039 F g^{-1}. We can use experimental values of the specific capacitance to estimate an average n value (electrons per Ru center) for each material reported. The maximum, for C_S=1,580 F g^{-1} in Table 3, is n~2.3, while the best value for the Ru oxide/CF composites is ~1.4.

Hu and Chen [39] have suggested that an n value of 4, for Ru(VI) to Ru(II), is possible over a 1.35 potential range, yielding a theoretical C_S of approximately 2,000 F g^{-1}. On the other hand, it has been shown by extended X-ray absorption fine structure that the main redox process for hydrous Ru oxide, which occurs over the potential range of approximately 0.25 to 1.05 V vs a reversible hydrogen electrode, involves only the one electron Ru(III) ↔ Ru(IV) process [52]. A second process does occur at higher potentials [52] but the reversible charge that can be passed is much less than for the Ru(III) ↔ Ru(IV) process. This high potential process only proceeds reversibly to a small extent before an irreversible oxidation begins to occur. This could be due to the instability or solubility of the Ru(V) or Ru(VI) that is formed and/or the onset of water oxidation. The Pourbaix diagram for Ru also indicates that only the Ru(III) and Ru(IV) oxides are stable under aqueous conditions. It therefore appears that the best n value that can be expected for Ru oxide is approximately 1.5, and this is the best that has been obtained for pure Ru oxide [7].

The very high Ru oxide specific capacitances reported by Hu and coworkers [24, 39] for their 10% Ru oxide/activated carbon composites appear to be anomalously high in light of the above discussion. A possible explanation for the high values is that the presence of Ru oxide increases the specific capacitance of the carbon support by oxidizing the surface to produce electroactive quinone-type functionality. This would increase the apparent specific capacitance of the Ru oxide since the subtraction of the capacitance due to the carbon would be too low. It is clear from the results in Fig. 4

that the capacitance of the carbon support can increase simply from exposure to 1 M H_2SO_4(aq), and the presence of Ru oxide was found to accelerate this process. We have attempted to correct for this by using C_S values for the CF after 17 h, but this may not be sufficient. There is clearly considerable uncertainty in determining the specific capacitance of low loadings of Ru oxide in composites. As the loading of Ru oxide is increased; however, any systematic error due to underestimation of the carbon contribution becomes smaller. This may account, in part, for the commonly observed decrease in the Ru oxide C_S with increasing loading.

Conclusions

Adsorption of colloidal Ru oxide onto high-surface-area carbon fabric has been shown to be an effective way to increase its specific capacitance in 1 M H_2SO_4(aq). The specific capacitances of the Ru oxide/CF composites increased with increasing Ru oxide loading with 427 F g^{-1} being obtained at 59% Ru oxide. The contribution from the Ru oxide was highest at the lowest loading (1,085 F/g at 9.15%). Impedance spectroscopy showed that the ionic conductivity of the electrodes was lower when Ru oxide was present, with the benefit being highest at the lowest Ru oxide loading. Consequently, the best power density of approximately 10 kW kg^{-1} was obtained at a loading of approximately 9% Ru oxide. The optimum energy density was 8.1 W h kg^{-1} at a Ru loading of approximately 20%.

Acknowledgements This work was supported by the Defense Research and Development Canada, the Natural Sciences and Engineering Council of Canada (NSERC), and Memorial University.

References

1. Frackowiak E (2007) Phys Chem Chem Phys 9:1774. doi:10.1039/b618139m
2. Burke A (2007) Electrochim Acta 53:1083. doi:10.1016/j.electacta.2007.01.011
3. Burke AF (2007) Proc IEEE 95:806. doi:10.1109/JPROC.2007.892490
4. Winter M, Brodd RJ (2004) Chem Rev 104:4245. doi:10.1021/cr020730k
5. Pandolfo AG, Hollenkamp AF (2006) J Power Sources 157:11. doi:10.1016/j.jpowsour.2006.02.065
6. Zheng JP, Cygan PJ, Jow TR (1995) J Electrochem Soc 142:2699. doi:10.1149/1.2050077
7. Liu X, Pickup PG (2008) J Power Sources 176:410. doi:10.1016/j.jpowsour.2007.10.076
8. Liu X, Pickup PG (2008) Energy Environ Sci 1:494
9. Zheng JP, Jow TR (1995) J Electrochem Soc 142:L6. doi:10.1149/1.2043984
10. Sugimoto W, Iwata H, Yokoshima K, Murakami Y, Takasu Y (2005) J Phys Chem B 109:7330. doi:10.1021/jp044252o
11. Santos MC, Terezo AJ, Fernandes VC, Pereira EC, Bulhoes LOS (2005) J Solid State Electrochem 9:91. doi:10.1007/s10008-004-0512-2
12. Foelske A, Barbieri O, Hahn M, Kotz R (2006) Electrochem Solid State Lett 9:A268. doi:10.1149/1.2188078
13. Jang JH, Kato A, Machida K, Naoi K (2006) J Electrochem Soc 153:A321. doi:10.1149/1.2138672
14. Kim IH, Kim KB (2006) J Electrochem Soc 153:A383. doi:10.1149/1.2147406
15. Sugimoto W, Yokoshima K, Murakami Y, Takasu Y (2006) Electrochim Acta 52:1742. doi:10.1016/j.electacta.2006.02.054
16. Fang WC, Huang JH, Chen LC, Su YLO, Chen KH (2006) J Power Sources 160:1506. doi:10.1016/j.jpowsour.2006.03.017
17. Juodkazis K, Juodkazyte J, Sukiene V, Griguceviciene A, Selskis A (2008) J Solid State Electrochem 12:1399. doi:10.1007/s10008-007-0476-0
18. Miller JM, Dunn B, Tran TD, Pekala RW (1997) J Electrochem Soc 144:L309. doi:10.1149/1.1838142
19. Zheng JP (1999) Electrochem Solid State Lett 2:359. doi:10.1149/1.1390837
20. Zhang JR, Jiang DC, Chen B, Zhu JJ, Jiang LP, Fang HQ (2001) J Electrochem Soc 148:A1362. doi:10.1149/1.1417976
21. Sato Y, Yomogida K, Nanaumi T, Kobayakawa K, Ohsawa Y, Kawai M (2000) Electrochem Solid State Lett 3:113. doi:10.1149/1.1390974
22. Kim H, Popov BN (2002) J Power Sources 104:52. doi:10.1016/S0378-7753(01)00903-X
23. Park JH, Ko JM, Park OO (2003) J Electrochem Soc 150:A864. doi:10.1149/1.1576222
24. Hu CC, Chen WC, Chang KH (2004) J Electrochem Soc 151:A281. doi:10.1149/1.1639020
25. Kim IH, Kim JH, Lee YH, Kim KB (2005) J Electrochem Soc 152:A2170. doi:10.1149/1.2041147
26. Wang YG, Wang ZD, Xia YY (2005) Electrochim Acta 50:5641. doi:10.1016/j.electacta.2005.03.042
27. Kim YT, Tadai K, Mitani T (2005) J Mater Chem 15:4914. doi:10.1039/b511869g
28. Min M, Machida K, Jang JH, Naoi K (2006) J Electrochem Soc 153:A334. doi:10.1149/1.2140677
29. Yu GY, Chen WX, Zheng YF, Zhao J, Li X, Xu ZD (2006) Mater Lett 60:2453. doi:10.1016/j.matlet.2006.01.015
30. Huang LM, Lin HZ, Wen TC, Gopalan A (2006) Electrochim Acta 52:1058. doi:10.1016/j.electacta.2006.06.040
31. Jang JH, Machida K, Kim Y, Naoi K (2006) Electrochim Acta 52:1733. doi:10.1016/j.electacta.2006.01.075
32. Choudhury NA, Shukla AK, Sampath S, Pitchumani S (2006) J Electrochem Soc 153:A614. doi:10.1149/1.2164810
33. Huang LM, Wen TC, Gopalan A (2006) Electrochim Acta 51:3469. doi:10.1016/j.electacta.2005.09.049
34. Lee BJ, Sivakkumar SR, Ko JM, Kim JH, Jo SM, Kim DY (2007) J Power Sources 168:546. doi:10.1016/j.jpowsour.2007.02.076
35. Hu CC, Wang CC, Chang KH (2007) Electrochim Acta 52:2691. doi:10.1016/j.electacta.2006.09.026
36. Fang WC, Leu MS, Chen KH, Chen LC (2008) J Electrochem Soc 155:K15. doi:10.1149/1.2801874
37. Pico F, Ibanez J, Lillo-Rodenas MA, Linares-Solano A, Rojas RM, Amarilla JM, Rojo JM (2008) J Power Sources 176:417. doi:10.1016/j.jpowsour.2007.11.001
38. Lee YH, Oh JG, Oh HS, Kim H (2008) Electrochem Commun 10:1035. doi:10.1016/j.elecom.2008.05.005
39. Hu CC, Chen WC (2004) Electrochim Acta 49:3469. doi:10.1016/j.electacta.2004.03.017
40. Niu JJ, Pell WG, Conway BE (2006) J Power Sources 156:725. doi:10.1016/j.jpowsour.2005.06.002
41. Hsieh C-T, Teng H (2002) Carbon 40:667. doi:10.1016/S0008-6223(01)00182-8
42. Andreas HA, Conway BE (2006) Electrochim Acta 51:6510. doi:10.1016/j.electacta.2006.04.045

43. Huang CW, Teng HS (2008) J Electrochem Soc 155:A739. doi:10.1149/1.2965503
44. Hu CC, Wang CC (2004) J Power Sources 125:299. doi:10.1016/j.jpowsour.2003.08.002
45. Jurewicz K, Babel K, Ziolkowski A, Wachowska H (2003) Electrochim Acta 48:1491. doi:10.1016/S0013-4686(03)00035-5
46. Hu CC, Li WY, Lin JY (2004) J Power Sources 137:152
47. Kalinathan K, DesRoches DP, Liu X, Pickup PG (2008) J Power Sources 181:182. doi:10.1016/j.jpowsour.2008.03.032
48. Frackowiak E, Beguin F (2001) Carbon 39:937. doi:10.1016/S0008-6223(00)00183-4
49. Kim Y-T, Ito Y, Tadai K, Mitani T, Kim U-S, Kim H-S, Cho B-W (2005) Appl Phys Lett 87:234106. doi:10.1063/1.2139839
50. Qu D (2002) J Power Sources 109:403. doi:10.1016/S0378-7753(02)00108-8
51. Miller JR (1998) 8th International Seminar on Double Layer Capacitors and Similar Energy Storage Devices, Deerfield Beach, Florida
52. Stefan IC, Mo Y, Antonio MR, Scherson DA (2002) J Phys Chem B 106:12373. doi:10.1021/jp026300f
53. Li HF, Wang RD, Cao R (2008) Microporous Mesoporous Mater 111:32. doi:10.1016/j.micromeso.2007.07.002